Published in final edited form as:
Radiat Res. 2005 November ; 164(5): 655–661.

Differential Impact of Mouse *Rad9* Deletion on Ionizing Radiation-Induced Bystander Effects

Aiping Zhu, **Hongning Zhou**, **Corinne Leloup**, **Stephen A. Marino**, **Charles R. Geard**, **Tom K. Hei**, and **Howard B. Lieberman**[1]
Center for Radiological Research, Columbia University College of Physicians and Surgeons, New York, New York 10032

Abstract

The cellular response to ionizing radiation is not limited to cells irradiated directly but can be demonstrated in neighboring “bystander” populations. The ability of mouse embryonic stem (ES) cells to express a bystander effect and the role of the radioresistance gene *Rad9* were tested. Mouse ES cells differing in *Rad9* status were exposed to broad-beam 125 keV/ μm ^{3}He α particles. All populations, when confluent, demonstrated a dose-independent bystander effect with respect to cell killing, and the *Rad9*$^{-}$/$^{-}$ genotype did not selectively alter that response or cell killing after direct exposure to this high-LET radiation. In contrast, relative to *Rad9*$^{+}$/$^{+}$ cells, the homozygous mutant was sensitive to direct exposure to α particles when in log phase, providing evidence of a role for *Rad9* in repair of potentially lethal damage. Direct exposure to α particles induced an increase in the frequency of apoptosis and micronucleus formation, regardless of *Rad9* status, although the null mutant showed high spontaneous levels of both end points. All populations demonstrated α-particle-induced bystander apoptosis, but that effect was most prominent in *Rad9*$^{-}$/$^{-}$ cells. Minimal α-particle induction of micro-nuclei in bystander cells was observed, except for the *Rad9*$^{-}$/$^{-}$ mutant, where a significant increase above background was detected. Therefore, the *Rad9* null mutation selectively sensitizes mouse ES cells to spontaneous and high-LET radiation-induced bystander apoptosis and micronucleus formation, but it has much less impact on cell killing by direct or bystander α-particle exposure. Results are presented in the context of defining the function of *Rad9* in the cellular response to radiation and its differential effects on individual bystander end points.

INTRODUCTION

It has recently been found that a biological response can be induced in cells neighboring those that are actually “hit” by radiation. This phenomenon has been called the bystander effect [for reviews see refs. (1, 2)]. This implies that cells directly exposed to radiation can transmit a signal to other cells nearby, thus in a sense amplifying the initial damage signal. In essence, this suggests that models taking into account only direct hits in mediating a biological response underestimate the true deleterious effects of radiation exposure,

[1]Address for correspondence: Center for Radiological Research, Columbia University College of Physicians and Surgeons, 630 W. 168th St., New York, NY 10032; lieberman@cancercenter.columbia.edu.

including potential health risks. Although the bystander effect was first implied from earlier work by Kotval and Gray (3), the modern-day definition was derived from more recent studies by Nagasawa and Little (4) when they reported that the calculated, expected nuclear traversal of 1% of cells in a population by a flux of α particles caused 30% of the cells to undergo sister chromatid exchanges. Subsequently, bystander effects have been demonstrated for cell survival, mutation and oncogenic transformation [for review see ref. (1)]. The use of a microbeam to target α particles to individual cells provides definitive evidence that a cell does not have to be hit directly by an α particle to demonstrate mutation or changes in survival. These experiments were performed using either one of two strategies. In the first, a lethal 20-hit dose of α particles could be delivered to 5% of the cells in a population, and mutations would arise in frequency similar to that observed when 100% of cells are hit with a single particle (5). Alternatively, Zhou *et al.* (6) showed that when 10% of a population was exposed to a single α particle, which is sublethal, many more cells in the population demonstrated chromosome aberrations and mutation than just the small percentage exposed. Interestingly, the mutation spectrum for bystander cells differed from that obtained spontaneously or after cytoplasmic irradiation, suggesting that different mutagenic mechanisms are involved (5).

Genetic makeup is important in terms of determining how a cell or individual will respond to radiation, and there is evidence that it can have an impact on the magnitude of the bystander effect produced. Nagasawa and Little (7) demonstrated that CHO cells deficient in DNA double-strand break repair (i.e., bearing an *xrs-5* mutation) show an enhanced chromosome aberration yield due to bystander effects induced by low fluences of α particles. They interpreted their results by stating that the *xrs-5* mutation reduced repair of double-strand DNA breaks caused by the α particles, and this prolonged a signal that mediates the bystander effect. However, beyond this finding, little is known about genetic mechanisms that underlie the bystander response to radiation.

The *rad9* gene was first identified in the fission yeast *Schizosaccharomyces pombe* (8, 9), and subsequently orthologs were found in humans [*RAD9* (10)] and mice [*Rad9* (11)]. The encoded protein plays a critical role in multiple pathways that respond to DNA damage. The human and mouse genes partially complement the sensitivity of *S. pombe rad9::ura4*$^{+}$ cells to ionizing radiation, UV radiation and the DNA synthesis inhibitor hydroxyurea (HU), as well as the associated cell cycle checkpoint defects. Homozygous *Rad9* knockout mouse ES cells are highly sensitive to ionizing radiation, UV radiation, and HU (12). In addition, they show defects in the maintenance of γ-ray-induced G_2/M checkpoint control. Wild-type *RAD9* or *Rad9* fully complements the sensitivity defects of the *Rad9*$^{-/-}$ mouse cells. The heterozygous *Rad9* knockout cells are also sensitive to at least ionizing radiation and HU. In addition, combined heterozygosity at both *Rad9* and *Atm* in mouse embryo fibroblasts alters cell transformation, apoptosis and DNA lesion repair dynamics (13), suggesting that human carriers of a mutation in one copy of *RAD9* might be genetically predisposed to the development of deleterious effects caused by DNA damage. In mammals, checkpoint genes are thought to maintain genomic stability, especially in the presence of DNA damage (14). Consistent with this, *Rad9*$^{-/-}$ mouse ES cells are genetically unstable and exhibit high frequencies of spontaneous chromosome aberrations and *Hprt* mutations (12). Also, *RAD9*

or *Rad9* restores genomic stability to the *Rad9*$^{-/-}$ cells. Therefore, when these evolutionarily conserved checkpoint genes are altered, genomic instability can occur and may lead to cancer (15).

In addition to roles in promoting resistance to DNA-damaging agents, cell cycle checkpoint control, and maintenance of genomic stability, pro-apoptosis activity has been demonstrated for at least the human and fission yeast RAD9 proteins (16, 17). Furthermore, Bessho and Sancar (18) reported that the human protein has 3′-5′ exonuclease activity. Yin and coworkers (19) demonstrated that RAD9 can regulate transcription of *CDKN1A* (*p21*) as well as other genes that may be part of a coordinately controlled damage response pathway. RAD9 can also stimulate the carbamoyl phosphate synthetase activity of CAD protein, which is required for *de novo* synthesis of pyrimidine nucleotides and cell growth (20), and interact with as well as stimulate the activity of multiple DNA repair proteins (21–24). Using a mouse model, *Rad9* was demonstrated to be essential for embryogenesis as well (12).

Since *Rad9* plays such a key role in multiple pathways important for cell growth and the response to DNA damage, we examined whether the gene functions in mediating radiation-induced bystander effects. Using an isogenic set of mouse embryonic stem cells differing in the status of *Rad9*, we found that alterations in the gene sensitize cells differentially to end points that reflect the bystander response. Ectopic expression of the wild-type human or mouse gene restores normal cellular function to the *Rad9*$^{-/-}$ mutant. Furthermore, we found that the ionizing radiation sensitivity promoted by a *Rad9* null mutation is dependent upon whether cells are actively growing or are confluent at the time of exposure.

MATERIALS AND METHODS

Cells and Culturing Conditions

The mouse embryonic stem cells used in this study and differing in the status of *Rad9* (*Rad9*$^{+}$/$^{+}$, *Rad9*$^{+}$/$^{-}$ *Rad9*$^{-}$/$^{-}$, *Rad9*$^{-}$/$^{-}$ ectopically expressing *Rad9*$^{+}$ or *RAD9*$^{+}$) were described previously (12). These cells were grown at 37°C in Knockout-DMEM (Invitrogen), with 15% ES-cell qualified fetal bovine serum, 0.1 m*M* non-essential amino acids, 2 m*M* L-glutamine, 10^{-4} *M* β-mercaptoethanol, 100 U/ml penicillin/streptomycin, and 1.0×10^{3}U/ml leukemia inhibitory factor (LIF, available as “ES-GRO” from Chemicon). Tissue culture plates and dishes were coated with a 0.1% gelatin solution and used routinely for cell passage and maintenance. Mylar dishes were coated with a 4-μg/ml fibronectin (Sigma) solution.

Bystander Experiments

Bystander studies were performed using a specialized two-ring system (Fig. 1). The outer stainless steel ring has a base made of Mylar that is 6 μm thick, and the inner ring contains several strips of 30 μm Mylar as a base. The outer and inner rings fit together. After sterilizing in 70% ethanol and air-drying, both Mylar layers were coated with fibronectin solution. ES cells (2.5×10^{5}) were plated onto the double Mylar culture rings. Two days later, cells were essentially 100% confluent, allowing direct cell-cell communication.

Confluent ES cells were irradiated with ^{3}He α particles (LET 120–125 keV/μm) or served as unirradiated controls. Dishes were irradiated from underneath using the track segment mode of a 4 MeV Van de Graaff accelerator located at the Radiological Research Accelerator Facility of Columbia University. Since α particles can penetrate the 6-μm but not the 30-μm Mylar, only cells growing on the lower, thinner surface were irradiated. However, the unirradiated cells on the 30-μm strips were in physical proximity to the irradiated cells and were the "bystander" population. After irradiation, the medium was immediately changed to remove dead floating cells, and the dishes were incubated for 24 h. Irradiated and unirradiated cells were removed from the 6-μm and 30-μm Mylar strips separately using trypsin. Part of the trypsinized culture was replated onto a two-well chamber slide coated with fibronectin for detecting micronuclei. Some of the culture was re-plated onto a 100-mm tissue culture dish coated with 0.1% gelatin for cell survival assays. Cells were also seeded onto a six-well plate to monitor apoptosis.

Cell Survival Assay

To determine resistance to 125 keV/μm α particles produced at the Columbia University Radiological Research Accelerator Facility, essentially completely confluent cells, as described in the previous section, were irradiated on 6-μm Mylar surfaces and then replated onto 100-mm dishes, followed by incubation for 7 to 10 days at 37°C. To test the sensitivity of actively growing populations to the charged particles, cells at up to 80% confluence after incubation for 24 h were trypsinized and plated (approximately 200 cells per dish) onto the 6-μm Mylar surfaces. After cells attached, usually 4–6 h after plating, they were irradiated and not replated. Medium for both experimental conditions was replaced with fresh Knockout-DMEM and supplements once during the postirradiation incubation period. Cells were then stained with 2% crystal violet and colonies were counted. Percentage survival was calculated as the number of colonies formed after irradiation relative to unirradiated controls × 100.

Apoptosis Assay

After treatment, cells (5×10^5) were seeded onto a six-well plate with fresh medium and incubated for 24 h. Cells were removed with trypsin, processed using the Annexin V-FITC apoptosis detection kit (Oncogene Research) following the manufacturer's instructions, and analyzed by flow cytometry with a FACSCalibur flow cytometer (Becton Dickinson). Floating cells were saved and scored, along with all others. Ten thousand cells were counted per point per experiment by flow cytometry, and each set of data is the average of at least three independent experiments.

Detection of Micronuclei

Irradiated or unirradiated cells were removed from the Mylar surface after 24 h using trypsin, plated on a two-well chamber slide containing supplemented Knockout-DMEM, and incubated for an additional 24 h. Cells were then fixed for 1 h to overnight with alcohol acid (95% ethanol/ 5% acetic acid). After fixation, slides were washed three times in PBS. After air-drying, the slides were stained with DAPI (Vector Laboratories). Cover slips were mounted onto the slides and cells were visualized using fluorescence microscopy. About 500 to 1000 cell nuclei were scored per sample.

Micronuclei were identified as being morphologically identical to but smaller than nuclei, and with the same staining intensity. They could touch but not overlap the main nucleus. Cells usually contain from zero to three micronuclei, but that number can occasionally be greater (25, 26). The assay was performed using published protocols (25, 27).

Statistics

Data points for cell survival, apoptosis and micronucleus assays represent the average of a minimum of three independent trials, and the standard errors of the means were calculated. In some instances, *t* tests were performed to determine whether differences between data points were statistically significant (i.e. ≤0.05).

RESULTS

Deletion of Rad9 does not Sensitize Confluent Cells to Killing by Direct or Bystander Exposure to Broad-Beam 125 keV/μm ^{3}He α Particles

Mouse embryonic stem cells null for *Rad9* and in log phase are sensitive to γ rays and UV light compared to control populations with wild-type *Rad9* (12). Therefore, the ability of 125 keV/μm ^{3}He α particles to selectively kill *Rad9*$^{-/-}$ cells after direct or bystander exposure when cells are confluent under standard conditions for bystander studies was tested. As indicated in Fig. 2A, all the populations were sensitive to direct exposure to this type of radiation, regardless of *Rad9* status. Furthermore, in contrast to previous results with γ rays or UV light using log-phase cells, the confluent *Rad9*$^{-/-}$ cells were no more sensitive to α particles than the confluent *Rad9*$^{+/+}$ or other *Rad9*$^{+}$ control populations. High levels of survival obtained especially at 5 and 10 Gy might be due to shielding in the confluent cultures.

The same set of mouse ES cells differing in *Rad9* status was examined for bystander cell killing due to α-particle exposure. As shown in Fig. 2B, confluent *Rad9*$^{+/+}$ mouse ES cells are sensitive to this type of radiation even when only neighboring cells are directly exposed. This is the first demonstration of a bystander effect in mouse ES cells. In addition, all the populations examined did not differ dramatically in the magnitude of this bystander response when compared at each dose ($P > 0.05$), indicating that loss of *Rad9* does not selectively sensitize mouse ES cells to bystander killing. A dose response for this end point was not observed, consistent with studies of other radiation-induced bystander effects (25, 28, 29),

Deletion of Rad9 Sensitizes Actively Growing Cells to 125 keV/μm ^{3}He α Particles

To determine whether the lack of a significant difference in sensitivity of *Rad9*$^{+/+}$ and *Rad9*$^{-/-}$ cells to α particles is because both populations were confluent at the time of radiation exposure, dose–response curves were established for these cells when irradiated as a confluent population or in log phase. Results indicate that *Rad9*$^{+/+}$ and *Rad9*$^{-/-}$ cells are equally sensitive to α particles when exposed as a confluent population (Fig. 3A), but the mutant is significantly more sensitive to this type of radiation when both populations are in log phase (Fig. 3B).

Spontaneous and 125 keV/μm ^{3}He α-Particle-Induced Apoptosis

The set of mouse ES cells with different *Rad9* genotypes was assessed for apoptosis. Figure 4A shows that all the populations demonstrated a spontaneous apoptosis frequency ranging from approximately 8 to 14%. Although this range was relatively narrow, *Rad9*$^{-/-}$ cells were at the high end. In addition, direct exposure to doses of α particles from 0.5 to 10 Gy induced higher frequencies of apoptotic cells in all the populations, as much as four times the background levels. At a dose above 5 Gy, there was no further increase in the frequency of apoptosis.

Deletion of Rad9 Sensitizes Cells to Bystander Apoptosis Caused by Broad-Beam 125 keV/μm ^{3}He α Particles

The role of *Rad9* in mediating radiation-induced bystander effects was tested further by examining apoptosis as an end point. Figure 4B shows that 125 keV/μm α particles in the dose range of 0.5 to 10 Gy can induce bystander apoptosis in all the populations. For most populations, 5 Gy induced peak frequencies of programmed cell death that were approximately double the spontaneous levels. The exception was the *Rad9*$^{-/-}$ cells ectopically expressing *RAD9,* where smaller increases in apoptosis frequencies, especially at 5 Gy, were observed. Also, the *Rad9*$^{-/-}$ population demonstrated the highest frequencies of apoptosis above background levels, and the spontaneous and induced levels were reduced when *Rad9* or *RAD9* was ectopically expressed in the homozygous mutant cells.

Spontaneous and 125 keV/μm ^{3}He α-Particle-Induced Micronucleus Formation

Micronucleus formation was examined in the same set of cells with different *Rad9* genotypes. Figure 5 indicates that spontaneous micronucleus frequencies in most populations ranged from 5 to 7%. However, *Rad9*$^{-/-}$ cells had two to three times that frequency, which was reduced by ectopic expression of either *Rad9* or *RAD9.* Alpha particles at doses of 0.5 to 10 Gy significantly increased the levels above background, with peak induction occurring at 5 Gy for all populations (Fig. 5A). Most data points for the *Rad9*$^{+/+}$ and *Rad9*$^{+/-}$ populations, as well as the *Rad9*$^{-/-}$ cells ectopically expressing *Rad9* or *RAD9,* differed statistically from the results for the *Rad9*$^{-/-}$ population ($P \leq 0.05$) but not from each other. Fig. 5A illustrates micro-nucleus formation 24 h postirradiation, but similar results were obtained 12 and 36 h post-treatment (data not shown). The only exception was when the 10-Gy points for the *Rad9*$^{-/-}$ cells and the same population with ectopic expression of the wild-type *Rad9* gene were compared ($P = 0.07$), due to the large error bars for the latter point.

Bystander Micronucleus Formation is Enhanced in Cells Deleted for Rad9

The ability of 125 keV/μm α particles to induce micro-nuclei in cells neighboring those directly irradiated was examined 24 h after exposure (Fig. 5B). With the exception of *Rad9*$^{-/-}$ cells, doses in the range of 0.5 to 10 Gy induced a minimal bystander effect, and usually any increase above background levels was not statistically significant. The largest increase was detected in the *Rad9*$^{-/-}$ cells, where 5 and 10 Gy induced statistically significant increases in bystander micronucleus formation above background levels. *Rad9*$^{-/-}$ cells ectopically expressing *Rad9* or *RAD9* did not demonstrate these high levels of

micronuclei. The levels of induced micronuclei were identical 12 and 36 h postirradiation (data not shown). Furthermore, differences in α-particle-induced cell cycle delays did not contribute to the results obtained since no delay was observed 24 h after treatment for *Rad9*$^{+/+}$ or *Rad9*$^{-/-}$ cells, as determined by flow cytometry (data not shown). Therefore, the *Rad9* null mutation sensitizes cells to α-particle-induced bystander micronucleus formation.

DISCUSSION

The bystander effect is a well-established phenomenon whereby cells neighboring those directly "hit" by radiation demonstrate a response typical of those actually exposed (1, 2). However, the molecular mechanisms that regulate this effect are not known. Mouse embryonic stem cells differing in the status of *Rad9* were used to determine whether this gene, which was previously found to play important roles in multiple fundamental cellular processes involving promotion of resistance to DNA damage and maintenance of genomic integrity (12), is an important element involved in regulating radiation-induced bystander effects. Using specially designed double Mylar dishes, we found that mouse ES cells can demonstrate bystander responses when neighboring cells are exposed to 125 keV/μm ^{3}He α particles. Interestingly, there were differences in the magnitude of the effects detected, depending on the end point monitored. For *Rad9*$^{+/+}$ cells, killing and the induction of apoptosis were readily detected in cells neighboring those "hit" by the α particles. In contrast, there was a minimal effect with respect to the induction of micronuclei in those bystander cells. *Rad9*$^{-/-}$ cells show bystander cell killing similar to the *Rad9*$^{+/+}$ population but more prominent induction of apoptosis and especially micronucleus formation. Since the level of induction of the individual end points differs within as well as between the *Rad9*$^{+/+}$ and *Rad9*$^{-/-}$ populations, the requirements to trigger bystander cell killing, apoptosis and micronucleus formation must not be exactly the same.

The *Rad9* null mutation sensitizes cells in particular to α-particle-induced bystander apoptosis and micronucleus formation. Previous studies demonstrated that an *xrs-5* mutation in CHO cells enhances chromosome aberration yields due to bystander effects caused by a low fluence of α particles (7). The investigators suggested that *xrs-5* reduced repair of α-particle-induced double-strand DNA breaks, resulting in prolongation of a signal that mediates the bystander effect. This may well be true also for the ability of *Rad9*$^{-/-}$ to enhance bystander apoptosis and micronucleus formation relative to the levels observed in *Rad9*$^{+/+}$ cells or *Rad9*$^{-/-}$ ectopically expressing *Rad9* or *RAD9*. In fact, recent studies with mouse embryo fibroblasts indicate that the *Rad9*$^{+/-}$ genotype alters the dynamics of DNA double-strand break repair (13). Other studies also support a role for the human version of the protein in regulating the efficiency of base excision repair (21–24). However, since the *Rad9* homozygous mutant did not selectively demonstrate enhanced bystander cell killing relative to that observed for the *Rad9*$^{+/+}$ population, the role of *Rad9* in mediating the different end points cannot depend upon the same signal in terms of quality and/or magnitude. *xrs-5* primarily causes deficiencies in DNA double-strand break repair, but *Rad9*$^{-/-}$ mediates problems not only with repairing damaged DNA but also with cell cycle checkpoint control, apoptosis and genomic stability. Whether the effects of *xrs-5* in CHO cells and *Rad9*$^{-/-}$ in mouse cells on the enhancement of individual bystander responses

reflect a common DNA damage repair defect, capable of modulating an initial bystander induction signal, or different mechanisms must await further analysis.

Spontaneous frequencies of apoptosis and especially micronuclei are high in *Rad9*$^{-/-}$ cell populations compared to *Rad9*$^{+/+}$ controls or the mutant ectopically expressing *Rad9* or *RAD9.* These findings are consistent with previous work demonstrating high spontaneous chromosome aberration and *Hprt* mutation frequencies in *Rad9*$^{-/-}$ cells (12) and further demonstrate a role for *Rad9* in maintaining genomic stability.

Human *RAD9* and *S. pombe rad9* cause programmed cell death when overexpressed in human cells and are thus considered pro-apoptosis proteins (16, 17). They each contain a BH3-like domain capable of binding the anti-apoptosis proteins BCL2 and BCL-XL. Furthermore, deletion of the BH3 domains neutralizes the pro-apoptosis function, as does co-expression of the anti-apoptosis gene *BCL2* with at least human *RAD9.* Interestingly, we demonstrate that *Rad9*$^{-/-}$ mouse ES cells show high levels of spontaneous and α-particle-induced apoptosis. Apoptosis frequencies were high in directly irradiated cells or in those not directly “hit” by α particles. This suggests that although *Rad9* has a pro-apoptosis function when overexpressed, it is not solely essential for the process. These results are consistent with the high frequency of apoptotic cells in E8.5 and E9.5 *Rad9*$^{-/-}$ mouse embryos (12). Furthermore, since *Rad9* has multiple functions, a defect might result in the accumulation of spontaneous DNA damage, as well as that induced by direct or bystander exposure to α particles, resulting in retention of damage and an apoptosis-inducing signal. An alternative explanation for the induction of apoptosis by *RAD9* overexpression but increased apoptosis in the absence of *Rad9* is that the mouse protein does not have pro-apoptosis activity. Although this function for *Rad9* was never tested, the lack of pro-apoptosis activity for the protein is unlikely since such a function was demonstrated for the human and fission yeast orthologs. In addition, the encoded mouse protein is structurally very similar to the *RAD9* gene product (11), and it also contains a BH3-like domain characteristic of pro-apoptosis proteins.

Mouse ES cells bearing *Rad9*$^{-/-}$ are no more sensitive to killing by 125 keV/μm α particles than *Rad9*$^{+/+}$ cells under the conditions used to test for bystander effects in which cells are confluent when irradiated. However, actively growing subconfluent *Rad9*$^{-/-}$ cells, relative to the isogenic *Rad9*$^{+/+}$ control, are more sensitive to this high-LET radiation. Previous studies indicated that actively growing *Rad9*$^{-/-}$ cells are much more sensitive to γ rays than the *Rad9*$^{+/+}$ population (12). These results suggest that the *Rad9*$^{-/-}$ cells may be defective in a repair process capable of mending potentially lethal damage. Commensurate with this, several investigators suggest a role for the human version of this protein in DNA repair (21–24).

In summary, radiation-inducible bystander responses have been demonstrated for mouse ES cells. Furthermore, cells containing *Rad9*$^{-/-}$ show an enhanced radiation-induced bystander effect for apoptosis and micronucleus formation, but not for cell killing, relative to the *Rad9*$^{+/+}$ population or related controls. These results suggest that *Rad9* is involved in mediating bystander effects, perhaps in the generation of an initiating signal, although the precise role for the protein has yet to be determined directly. Our findings also suggest that

individual bystander responses have different requirements for activation since the magnitude of induction within and between the *Rad9*$^{+/+}$ and *Rad9*$^{-/-}$ populations for each bystander-related end point was different even after cells were exposed to the same doses of radiation before analysis. More studies are clearly needed to define the molecular mechanisms that mediate bystander responses. Results gleaned from such investigations are sure to have an impact on calculating risk assessment after ionizing radiation exposure, in particular in terms of understanding contributions made by tissues adjacent to but not directly in a radiation field.

Acknowledgments

We thank Adayabalam S. Balajee for technical advice related to the detection of micronuclei and Gary Johnson for providing the picture of the Mylar dishes. This work was supported by NIH grants CA89816 and GM52493 to HBL, CA75061 to CRG, and CA49062 and ES12888, as well as DOE grant 98ER62687 to TKH. The Radiological Research Accelerator Facility of Columbia University was supported by NIH grant EB002033.

References

1. Morgan WF. Non-targeted and delayed effects of exposure to ionizing radiation: II. Radiation-induced genomic instability and bystander effects *in vivo*, clastogenic factors and transgenerational effects. Radiat Res. 2003; 159:581–596. [PubMed: 12710869]
2. Morgan WF. Non-targeted and delayed effects of exposure to ionizing radiation: I. Radiation-induced genomic instability and bystander effects *in vitro*. Radiat Res. 2003; 159:567–580. [PubMed: 12710868]
3. Kotval JP, Gray LH. Structural changes produced in microspores of *Tradescantia* by α-particles. J Genet. 1947; 48:135–154. [PubMed: 20266728]
4. Nagasawa H, Little JB. Induction of sister chromatid exchanges by extremely low doses of alpha-particles. Cancer Res. 1992; 52:6394–6396. [PubMed: 1423287]
5. Zhou H, Randers-Pehrson G, Waldren CA, Vannais D, Hall EJ, Hei TK. Induction of a bystander mutagenic effect of alpha particles in mammalian cells. Proc Natl Acad Sci USA. 2000; 97:2099–2104. [PubMed: 10681418]
6. Zhou H, Suzuki M, Randers-Pehrson G, Vannais D, Chen G, Trosko JE, Waldren CA, Hei TK. Radiation risk to low fluences of alpha particles may be greater than we thought. Proc Natl Acad Sci USA. 2001; 98:14410–14415. [PubMed: 11734643]
7. Nagasawa H, Little JB. Bystander effect for chromosomal aberrations induced in wild-type and repair deficient CHO cells by low fluences of alpha particles. Mutat Res. 2002; 508:121–129. [PubMed: 12379467]
8. Murray JM, Carr AM, Lehmann AR, Watts FZ. Cloning and characterisation of the *rad9* DNA repair gene from *Schizosaccharomyces pombe*. Nucleic Acids Res. 1991; 19:3525–3531. [PubMed: 1852603]
9. Lieberman HB, Hopkins KM, Laverty M, Chu HM. Molecular cloning and analysis of *Schizosaccharomyces pombe rad9*, a gene involved in DNA repair and mutagenesis. Mol Gen Genet. 1992; 232:367–376. [PubMed: 1588907]
10. Lieberman HB, Hopkins KM, Nass M, Demetrick D, Davey S. A human homologue of the *Schizosaccharomyces pombe rad9*$^{+}$ checkpoint control gene. Proc Natl Acad Sci USA. 1996; 93:13890–13895. [PubMed: 8943031]
11. Hang H, Rauth SJ, Hopkins KM, Davey SK, Lieberman HB. Molecular cloning and tissue-specific expression of *Mrad9*, a murine orthologue of the *Schizosaccharomyces pombe rad9*$^{+}$ checkpoint control gene. J Cell Physiol. 1998; 177:241–247. [PubMed: 9766521]
12. Hopkins KM, Auerbach W, Wang XY, Hande MP, Hang H, Wolgemuth DJ, Joyner AL, Lieberman HB. Deletion of mouse *rad9* causes abnormal cellular responses to DNA damage, genomic instability and embryonic lethality. Mol Cell Biol. 2004; 24:7235–7248. [PubMed: 15282322]

13. Smilenov LB, Lieberman HB, Mitchell SA, Baker R, Hopkins KM, Hall EJ. Combined haploinsufficiency for *ATM* and *RAD9* as a factor in cell transformation, apoptosis and DNA lesion repair dynamics. Cancer Res. 2005; 65:933–938. [PubMed: 15705893]
14. Bartkova J, Lukas J, Bartek J. Aberrations of the G1- and G1/ S-regulating genes in human cancer. Prog Cell Cycle Res. 1997; 3:211–220. [PubMed: 9552416]
15. Hartwell LH, Kastan MB. Cell cycle control and cancer. Science. 1994; 266:1821–1828. [PubMed: 7997877]
16. Komatsu K, Miyashita T, Hang H, Hopkins KM, Zheng W, Cuddeback S, Yamada M, Lieberman HB, Wang H-G. Human homologue of *S. pombe* Rad9 interacts with Bcl-2/Bcl-xL and promotes apoptosis. Nat Cell Biol. 2000; 2:1–6. [PubMed: 10620799]
17. Komatsu K, Hopkins KM, Lieberman HB, Wang H-G. *Schizosaccharomyces pombe* Rad9 contains a BH3-like region and interacts with the anti-apoptotic protein Bcl-2. FEBS Lett. 2000; 481:122–126. [PubMed: 10996309]
18. Bessho T, Sancar A. Human DNA damage checkpoint protein hRAD9 is a 3′ to 5′ exonuclease. J Biol Chem. 2000; 275:7451–7454. [PubMed: 10713044]
19. Yin Y, Zhu A, Jin YJ, Liu YX, Zhang X, Hopkins KM, Lieberman HB. Human RAD9 checkpoint control/proapoptotic protein can activate transcription of *p*21. Proc Natl Acad Sci USA. 2004; 101:8864–8869. [PubMed: 15184659]
20. Lindsey-Boltz LA, Wauson EM, Graves LM, Sancar A. The human Rad9 checkpoint protein stimulates the carbamoyl phosphate synthetase activity of the multifunctional protein CAD. Nucleic Acids Res. 2004; 32:4524–4530. [PubMed: 15326225]
21. Wang W, Brandt P, Rossi ML, Lindsey-Boltz L, Podust V, Fanning E, Sancar A, Bambara RA. The human Rad9-Rad1-Hus1 checkpoint complex stimulates flap endonuclease 1. Proc Natl Acad Sci USA. 2004; 101:16762–16767. [PubMed: 15556996]
22. Helt CE, Wang W, Keng PC, Bambara RA. Evidence that DNA damage detection machinery participates in DNA repair. Cell Cycle. 2005; 4:529–532. [PubMed: 15876866]
23. Smirnova E, Toueille M, Markkanen E, Hübsche U. The human checkpoint sensor and alternative DNA clamp Rad9/Rad1/Hus1 modulates the activity of DNA ligase I, a component of the long patch base excision repair machinery. Biochem J. 2005; 389:13–17. [PubMed: 15871698]
24. Toueille M, El-Andaloussi N, Frouin I, Freire R, Funk D, Shevelev I, Friedrich-Heineken E, Villani G, Hottiger MO, Hubscher U. The human Rad9/Rad1/Hus1 damage sensor clamp interacts with DNA polymerase beta and increases its DNA substrate utilisation efficiency: implications for DNA repair. Nucleic Acids Res. 2004; 32:3316–3324. [PubMed: 15314187]
25. Prise KM, Belyakov OV, Folkard M, Michael BD. Studies of bystander effects in human fibroblasts using a charged particle microbeam. Int J Radiat Biol. 1998; 74:793–798. [PubMed: 9881726]
26. Fenech M. The *in vitro* micronucleus technique. Mutat Res. 2000; 455:81–95. [PubMed: 11113469]
27. Ponnaiya B, Jenkins-Baker G, Brenner DJ, Hall EJ, Randers-Pehrson G, Geard CR. Biological responses in known bystander cells relative to known microbeam-irradiated cells. Radiat Res. 2004; 162:426–432. [PubMed: 15447040]
28. Limoli CL, Ponnaiya B, Corcoran JJ, Giedzinski E, Kaplan MI, Hartmann A, Morgan WF. Genomic instability induced by high and low LET ionizing radiation. Adv Space Res. 2000; 25:2107–2117. [PubMed: 11542863]
29. Yang H, Asaad N, Held KD. Medium-mediated intercellular communication is involved in bystander responses of X-ray-irradiated normal human fibroblasts. Oncogene. 2005; 24:2096–2103. [PubMed: 15688009]

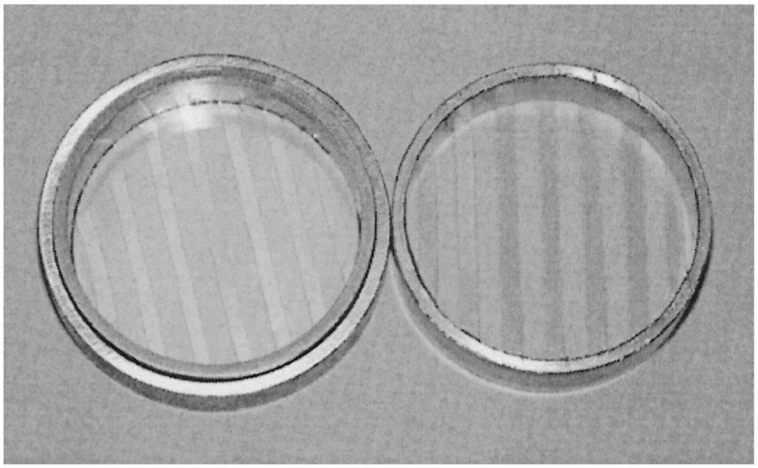

FIG. 1.

Double ring Mylar dishes used for bystander studies. Left: Photograph shows the outer stainless steel ring with a base made of Mylar that is 6 μm thick, and contained within is the inner ring bearing several strips of 30-μm Mylar as a base. The outer and inner rings fit together. Right: The inner ring with strips of Mylar.

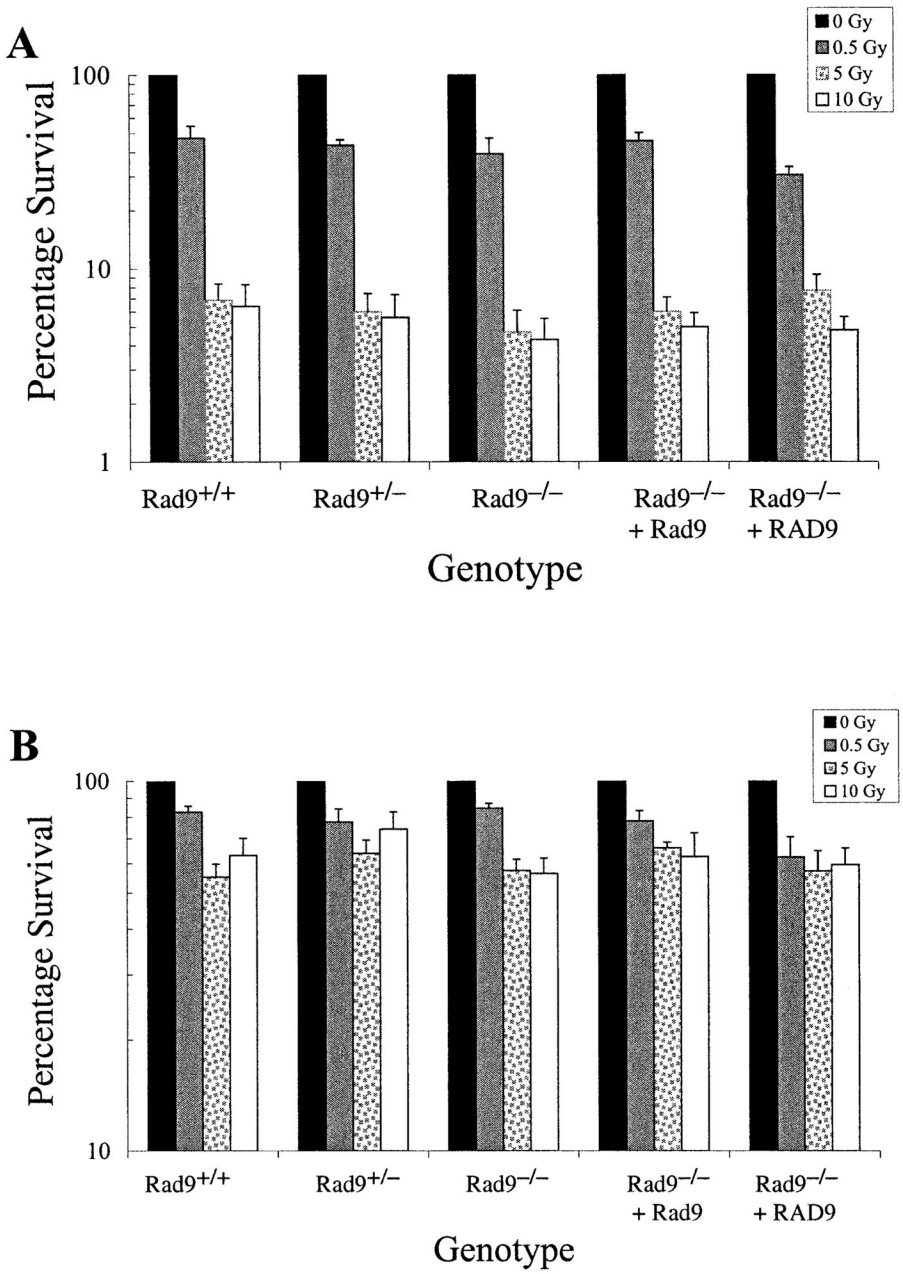

FIG. 2.

Cell survival after exposure to broad-beam 125 keV/μm ^{3}He α particles. Panel A: Colony formation after direct exposure to 0, 0.5, 5 or 10 Gy of α particles. Panel B: Colony formation after bystander exposure to the doses indicated above. The mouse ES cell populations used have the following genotypes: *Rad9*$^{+}$/$^{+}$, *Rad9*$^{+}$/$^{-}$, *Rad9*$^{-}$/$^{-}$, *Rad9*$^{-}$/$^{-}$ ectopically expressing *Rad9*, *Rad9*$^{-}$/$^{-}$ ectopically expressing *RAD9*. Columns represent the average of three independent experiments ±SEM as indicated.

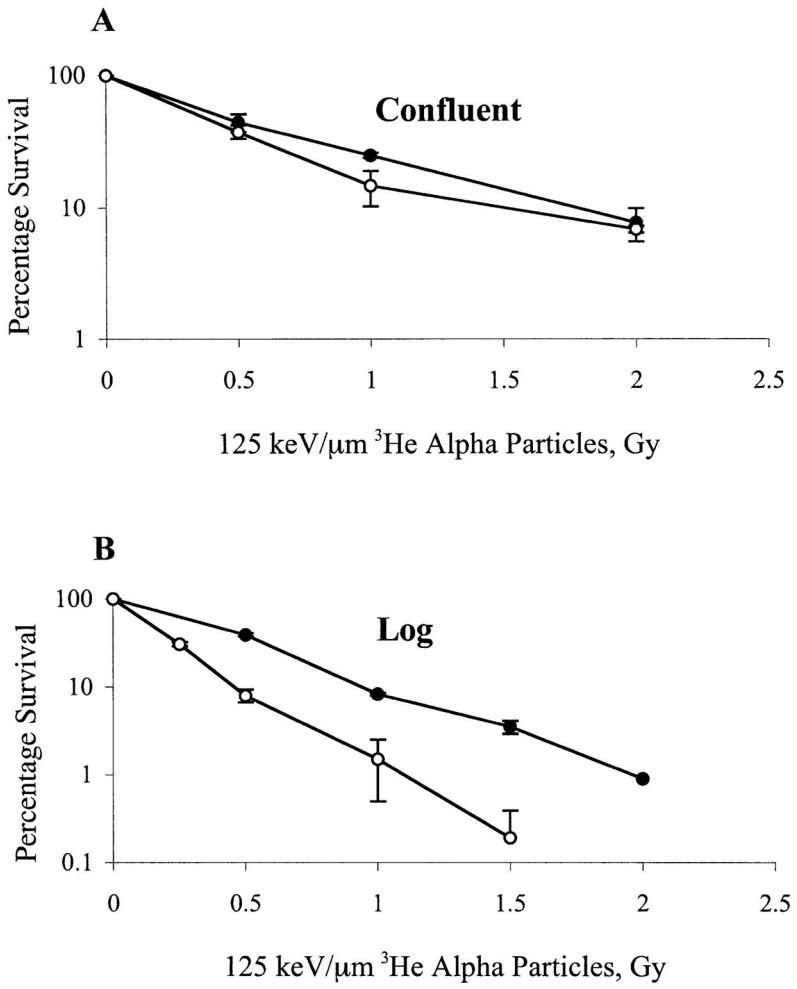

FIG. 3.

Effects of growth status on cell survival after direct exposure to 125 keV/μm ^{3}He α particles. Panel A: Confluent cells exposed to α particles. Panel B: Actively growing cells exposed to α particles. Mouse ES cell populations used have the following genotypes: *Rad9*$^{+}$/$^{+}$ (closed circles), *Rad9*$^{-}$/$^{-}$ (open circles). Points represent the average of at least three experiments ±SEM as indicated.

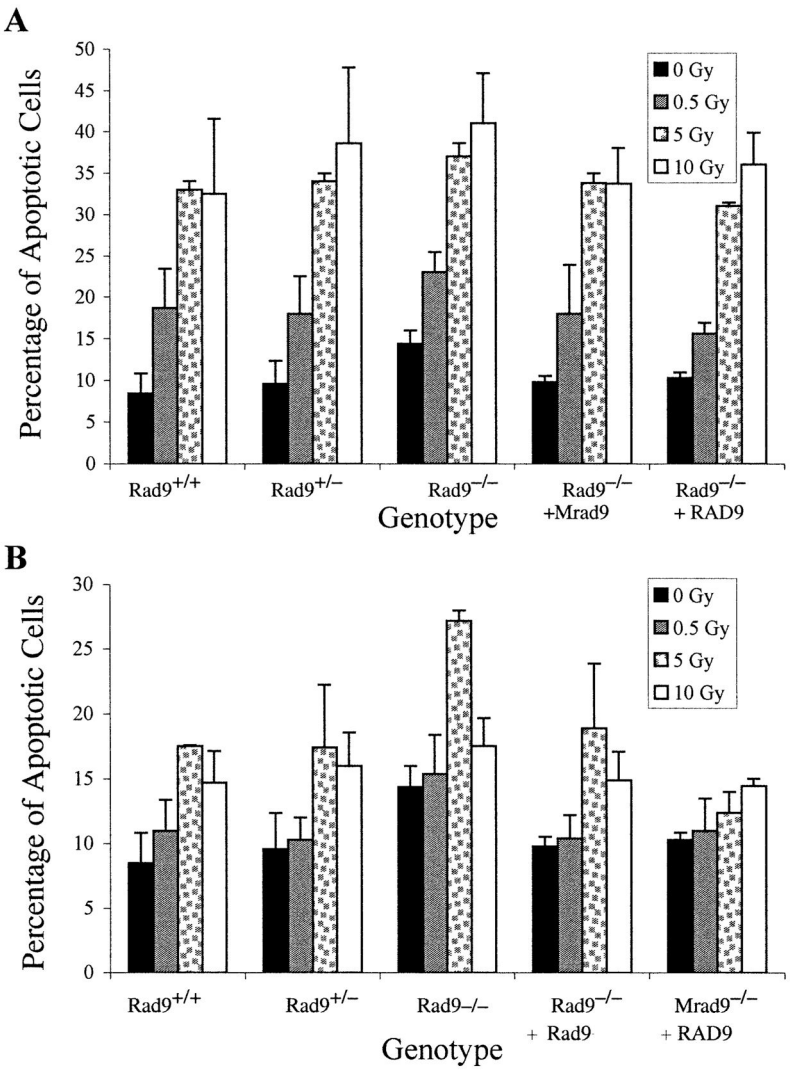

FIG. 4.

Induction of apoptosis by 125 keV/μm ^{3}He α particles. Panel A: Apoptosis after direct exposure to 0, 0.5, 5 or 10 Gy of α particles. Panel B: Apoptosis after bystander exposure to the doses indicated above. Mouse ES cell populations used have the following genotypes: *Rad9*$^{+}$/$^{+}$, *Rad9*$^{+}$/$^{-}$, *Rad9*$^{-}$/$^{-}$, *Rad9*$^{-}$/$^{-}$ ectopically expressing *Rad9*, *Rad9*$^{-}$/$^{-}$ ectopically expressing *RAD9*. Columns represent the average of three independent experiments ±SEM as indicated.

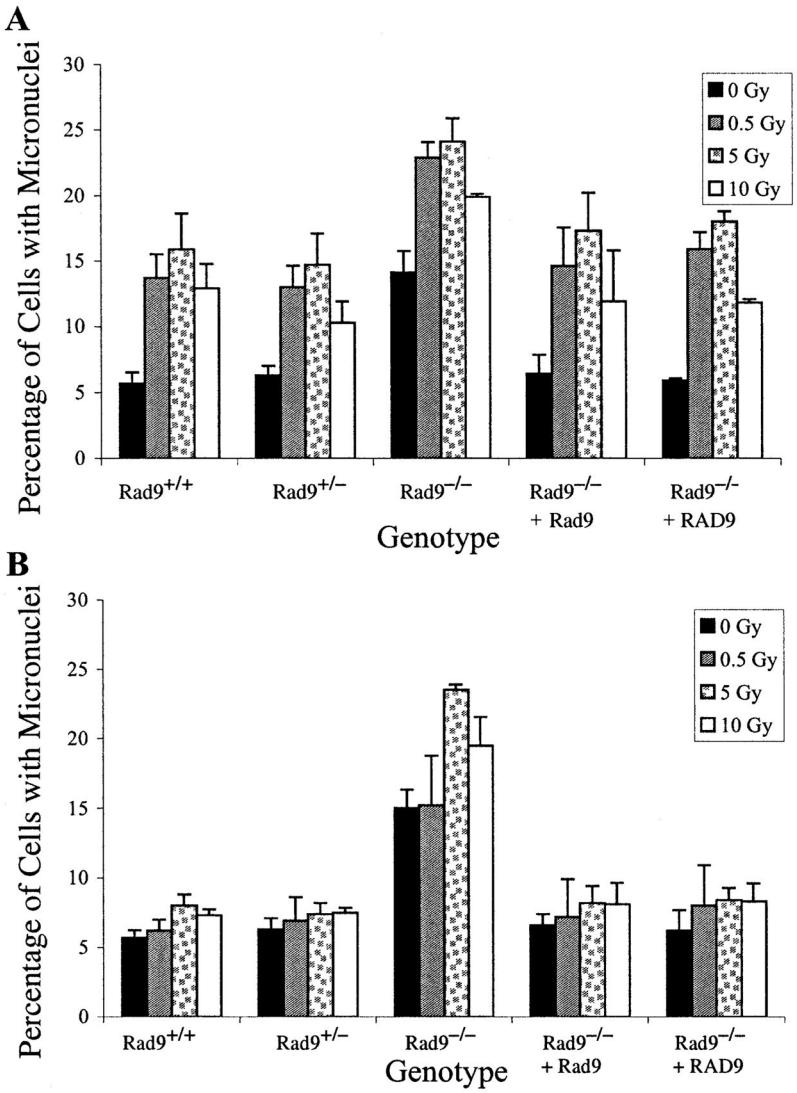

FIG. 5.

Induction of micronuclei by 125 keV/μm ^{3}He α particles. Panel A: Micronucleus formation after direct exposure to 0, 0.5, 5 or 10 Gy of α particles. Panel B: Micronucleus formation after bystander exposure to the doses indicated above. Mouse ES cell populations used have the following genotypes: *Rad9*$^{+}$/$^{+}$, *Rad9*$^{+}$/$^{-}$, *Rad9*$^{-}$/$^{-}$, *Rad9*$^{-}$/$^{-}$ ectopically expressing *Rad9*, *Rad9*$^{-}$/$^{-}$ ectopically expressing *RAD9*. Columns represent the average of three independent experiments ±SEM as indicated.